

H. Springer et al.: A novel roll-bonding methodology for the cross-scale analysis of phase properties and interactions

Hauke Springer, Cem Tasan, Dierk Raabe

Max-Planck-Institut für Eisenforschung GmbH, Düsseldorf, Germany

A novel roll-bonding methodology for the cross-scale analysis of phase properties and interactions in multiphase structural materials

We introduce a new thermo-mechanical approach for producing layered bulk samples built-up from the constituent phases of structural materials for the analysis of multiphase co-deformation phenomena. Following a thermo-mechanically controlled roll-bonding procedure, the intrinsic properties of the microstructural components as well as their mutual mechanical interaction and interfacial phenomena can be systematically investigated in highly controlled model microstructures of reduced complexity. The effectiveness of the approach is demonstrated on two examples where austenite or martensite layers, respectively, are introduced in a bulk ferritic matrix, representing in either case components of high strength steels. Special emphasis is laid on how the plasticity of martensite within ferrite, as a key parameter required for understanding and optimising dual phase steels, can be investigated following the proposed approach.

Keywords: Multiphase materials; Steels; Dual-phase steel; Microstructure design; Micro-mechanical testing

1. Introduction

Novel structural materials with optimised mechanical properties often consist of a variety of phases, with the aim of achieving desirable bulk properties through a favourable interaction of the specific microstructure constituents. This

approach is especially important in the alloy design of advanced high strength steels, whose properties can be tailored for specific applications, e. g. in lightweight transportation systems [1–3]. Examples are dual-phase (DP) or transformation induced plasticity (TRIP) assisted steels, which rely on martensite, bainite and/or various carbides to strengthen a ductile ferritic and/or austenitic matrix [4–6]. These composite-like microstructures lead to good formability, high energy absorption upon crashing and increased strength. Note that the latter property enables reduction of wall thickness and hence, weight of, e. g. an automotive bodyshell (body-in-white) as well [7–9]. These multiphase microstructures are typically achieved by appropriate alloying strategies and adapted thermo-mechanical processing parameters, such as controlled cooling after intercritical annealing, the effects of which are often reinforced by partitioning of alloying elements [1, 10, 11].

It should be noted, however, that in most cases the alloy/microstructure design process is guided by pursuing trends in the global mechanical properties (top-down), rather than by a systematic assessment and optimisation of the characteristics of the underlying individual phases and their micro-mechanical interactions (bottom-up). The reason for this approach is that the microstructures in many multiphase materials, especially steels, are very complex regarding not only the types of phases, but also their crystallography, volume fraction, morphology, interfaces, and dispersion, as well as their intrinsic properties and their interaction during deformation [2, 12]. Additionally, the different properties of the components can be mutually dependent, e. g. the plas-

tivity of a dispersed phase may change along with its size or the strength of the surrounding matrix [13]. Despite the strong motivation for further optimisation of the mechanical performance of advanced steels, the complexity presented above, and the typical sub-micron size of the embedded non-matrix phases (e. g. martensite in DP steels [13, 14], reverted austenite in ultra-high strength martensitic steels [15, 16] etc.) render an accurate assessment of individual phase properties and their contribution to bulk properties complicated, thus making systematic studies unfeasible.

To this end, two approaches are typically followed: micro-testing samples of decreased dimensions (i. e. through indentation or pillar compression tests), or macro-testing microstructures of enlarged dimensions (i. e. produced through crystal growth). The former approach has provided tremendous insight regarding the understanding of fundamental mechanisms of plasticity [17, 18]. However, limiting sample dimensions in the micro- or nano-scales lead to intrinsic incapability in mapping the full extent of the hierarchical deformation processes occurring in complex bulk phase configurations, where strain distribution and microstructural heterogeneity span over many scales [19]. The latter approach can overcome this difficulty, however only for those special cases in which the production of bulk crystals of two (or more) phases in the required chemical and crystallographic configuration is possible.

Thus, in order to simplify the investigation of these complex micro-mechanical phenomena, it is of high interest to develop alternative experimental methodologies to create sufficiently large bulk multiphase samples with controlled geometry, constitutions and overall microstructures. Building on the recently expanding field of multi-layered material synthesis, we propose in this work a novel methodology that

- (i) provides such bulk samples consisting of the constituting phases of structural materials; and
- (ii) allows practical characterisation of co-deformation of these phases across different length scales. To demonstrate how the intrinsic properties of microstructural components and their mutual interactions can be investigated in a well-defined model microstructure of reduced complexity, this methodology has been applied to two examples, namely, micron-sized austenite and martensite layers, respectively, both embedded in ferritic matrices. It should be emphasized that this work is not directed at studying the basics of the roll-bonding method but uses this approach to design simple model microstructures for conducting a systematic phase co-deformation analysis. The insights obtained from using this method better enable knowledge-based design and optimisation of multiphase structural materials.

2. Methods and materials

2.1. Multi-layered material synthesis

Different routes have been pursued in the literature for the synthesis of multi-layered metallic materials [20, 21]. Following a “bottom-up” approach, physical or chemical vapour deposition techniques [22, 23] have been employed to produce multilayered materials with highly controllable chemical concentration profiles throughout the specimen. These techniques have found use in studying interfacial

phenomena down to the nano-scale, e. g. in the copper–niobium system [22]. The main limitations of this approach are the increased experimental effort and small sample dimensions. Replacing sputtering techniques with thermal coating procedures such as plasma-spraying or laser metal deposition greatly increases the deposition rate and thus the achievable sample size, but also the minimum layer thickness, and the interface between the layers shows all the – here unwanted – characteristics of a fusion weld, i. e. intermixing in the meltpool and presence of surrounding heat affected zones [24, 25].

Another approach to achieve hybrid microstructure materials is to perform surface modifications of bulk samples via thermal treatments such as laser hardening [26] or mechanical processing [27]. Both techniques are fast and easily applied to larger sample dimensions, but are limited in the possible chemical variations and also in changing independently from another the geometry (such as layer thickness) and type (e. g. amount of induced deformation) of the modified surface regions.

In this light, using roll bonding as a “top-down” approach to join materials of different chemical composition and thickness appears favourable, as it allows for the rapid generation of large bulk samples with minimised effort, and is highly controlled in terms of geometry and location of the layers [28–31]. Roll bonding is a solid-state, pressure welding technique, where two or more metallic materials (similar or dissimilar) are stacked on top of each other and then fed through a rolling mill. The required amount of induced deformation is reduced by increased joining temperature as well as by improved smoothness and cleanliness of the contact surfaces. Thickness and microstructure of individual layers in the finished strip depend on

1. the initial build-up and composition profile of the stack
2. respective deformation of the chosen materials; and
3. the parallel or post-synthesis heat-treatments.

These steps are effectively the equivalent of the thermo-mechanical processing applied in contemporary alloy processing routes, and likewise, provide significant room for optimisation of mechanical behaviour of the multilayered bulk sheets [32, 33].

Roll bonding has therefore found widespread use for industrial production of large quantities of bi- or even multi-metallic sheets and strips, applied, e. g. in electrical contacts or thermally activated switches [34, 35]. Most works are concerned with achieving superior mechanical or physical properties, e. g. by roll bonding strong martensitic steel (low alloyed, high carbon (C) content) with highly ductile and corrosion resistant austenitic stainless steel [33, 36, 37]. Others aim at inducing massive deformation by accumulative bonding at low temperature [28, 38]. However, the technique has not yet been exploited for the targeted combination of materials representing components of multiphase bulk high strength steels.

2.2. Production of samples

The chemical composition (wt.%, wet chemical analysis) of the iron (Fe)-based materials chosen for the experiments in this study are listed in Table 1. The materials are referred to throughout the manuscript by the respective abbreviations given in the table. From the hot-rolled base materials,

blocks with 50 mm length, 30 mm width and varying thickness (see below) were prepared by spark erosion. The $30 \times 50 \text{ mm}^2$ contact surfaces were machine-ground to 1000 grit and degreased using an ultrasonic bath of ethanol and acetone. After stacking blocks of different materials they were tungsten inert gas (TIG) welded all around. Bonding was performed by annealing the stacked blocks at 1100°C for 10 min, followed by one rolling pass with a reduction of about 40% (roll speed about 5 cm s^{-1}) and direct water quenching. The TIG welds sealed the contact surface from the atmosphere to prevent excessive formation of oxide scales on the contact surfaces during heating to the bonding temperature. Water quenching directly after bonding limits interdiffusion between the now intimately joined materials of different chemical composition, ensuring well defined interface geometry.

Two exemplary types of samples were fabricated in this work, namely, ferrite–martensite–ferrite and ferrite–austenite–ferrite. The respective thermodynamic data of the processing procedure is sketched in Fig. 1:

(1) In order to obtain an austenite layer in a ferrite matrix, a 1 mm thick Fe40Ni sheet was placed between two 10 mm thick Fe blocks, bonded by the aforementioned procedure and then jointly cold-rolled to a final thickness of 1 mm (total engineering thickness reduction of 95.23%). Such high reductions after the bonding procedure are not only required to achieve a thin layer thickness of the final material sheets, but it is also helpful to improve the quality of the bonded interface by breaking up, dispersing and smoothing out any initial interface imperfections such as oxide films or scratches [32, 39]. Work hardening induced by the cold-rolling was removed by annealing at 700°C for 10 min followed by water quenching to room temperature. As can be seen from the section of the sketched Fe–Ni phase diagram shown in Fig. 1a, the Fe40Ni material is fully austenitic at 700°C while Fe remains ferritic, thus limiting Ni interdiffusion between the bonded materials. By repeating the bonding procedure with already bonded sheets as starting materials, a variation and combination of different layer thickness was achieved.

(2) Martensite layers within a ferrite matrix were created by bonding a Fe0.2C sheet between two blocks of Fe2Si following the above described procedure. Different volume fractions of martensite (5, 10, 20 and 50 vol.%) were achieved using appropriate thickness ratios of the Fe2Si and Fe0.2C base materials. After the bonding pass, the samples were isothermally hot rolled at 920°C to a thickness of $\sim 1 \text{ mm}$ and quenched in water. The final microstructure was obtained by annealing 900°C for 10 min and water quenching. As can be seen in Fig. 1b from the sketches of the Fe–C (right) and Fe–Si phase diagram (left), Fe2Si is

Table 1. Actual chemical compositions in wt.% obtained by wet chemical analysis of the materials used in this study.

Material	Actual composition (wt.%)
Fe	0.02 Ni, 0.004 Si, 0.007 C, balance Fe
Fe40Ni	39.8 Ni, balance Fe
Fe2Si	1.93 Si, balance Fe
Fe0.2C	0.224 C, balance Fe

ferritic between 900 and 920°C while Fe0.2C is austenitic. Similar to the partitioning process in a DP steel, this annealing procedure aimed at minimising C diffusion into the Si alloyed material, and thus at retaining a well defined interface between the two phase layers [40, 41].

In both cases (Fe/Fe40Ni/Fe; Fe2Si/Fe0.2C/Fe2Si), no additional films or interlayers between the joined materials were used, as they may aid bonding but eliminate the possibility to form a “natural” interface (interfacial energies, orientation relationships etc.) as between the components within a complex bulk structural material.

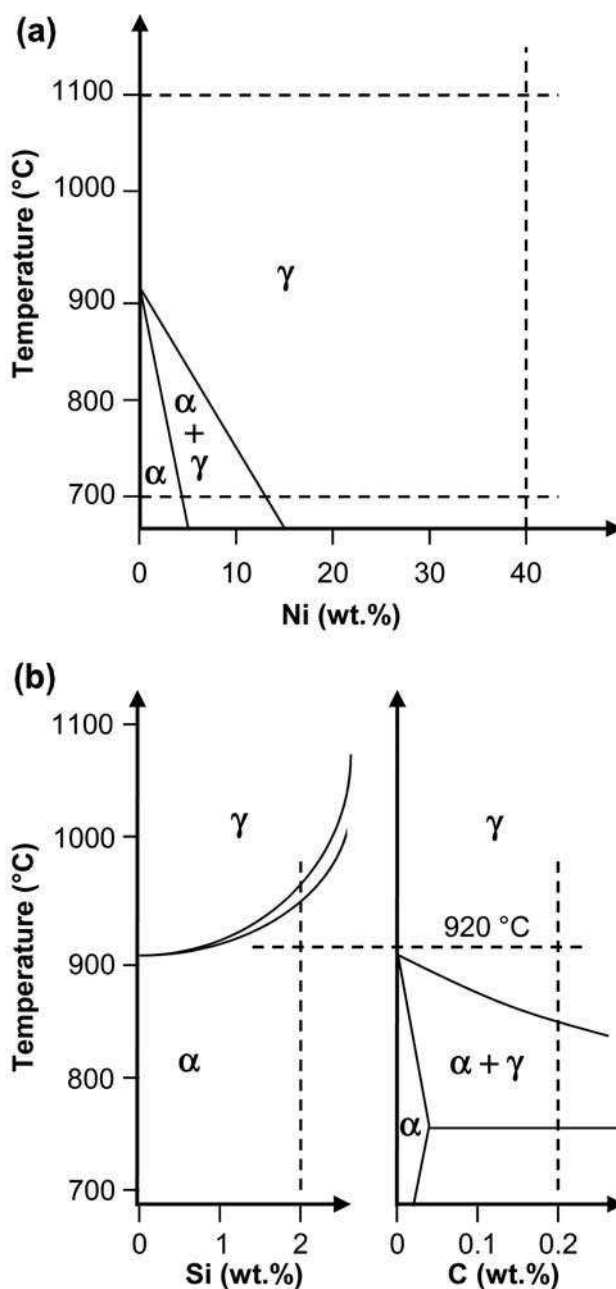


Fig. 1. Sketched sections of the phase diagrams for the two different material combinations: (a) Fe–Ni system, (b) Fe–Si and Fe–C systems. Processing temperatures and chemical concentrations are highlighted by the dashed lines.

2.3. Characterisation

For both sample types, optical microscopy (OM) was performed on cross and longitudinal sections after grinding and polishing with standard metallographic techniques using a Zeiss Axiophot 1. Scanning electron microscopy (SEM) analysis with a Jeol 6500F at 15 kV was carried out on cross-sections using energy dispersive X-ray (EDX, EDAX Genesis software) and electron backscatter diffraction analysis (EBSD, TSL OIM software). Chemical concentration profiles and micro-hardness measurements (HV0.01) on cross-sections of the ferritic/martensitic specimens were obtained by electron probe micro analysis (EPMA, Jeol JXA-8100) and a Fischerscope indenter, respectively.

To investigate deformation-induced evolution of the multi-layered microstructures, tensile tests were carried out, as schematically described in Fig. 2. Dog-bone-shaped tensile samples were produced by spark erosion (gauge length 5 mm, parallel to the rolling direction). A graphite black speckle pattern on a chalk white base (average speckle size 101.6 μm) was applied on the surface (rolling plane) of the specimens for digital image correlation (DIC) based local strain field measurements. The tensile tests were carried out on a Kammrath and Weiss tensile stage with an initial strain rate of 2×10^{-3} . DIC analysis was carried out employing an Aramis system (GOM GmbH Germany; software version 6.3, facet size 19 pixel, step size 15 pixel, 9.7 μm per pixel, 1 frame s^{-1}). Following the tensile tests, microstructural characterisation was carried out on longitudinal sections of the tensile specimen at locations of known local strain levels.

3. Results

3.1. Microstructural characterisation of the bonded materials

Optical images of as-processed microstructures, i.e. without the final recrystallisation or austenitisation and quenching treatment, are shown in Fig. 3 at different magnifications. Cross-sections are shown on the left side,

longitudinal sections on the right side, respectively. For both compounds, Fe/Fe40Ni/Fe (Fig. 3a) and Fe2Si/Fe0.2C/Fe2Si (Fig. 3b), an intermediate layer with a thickness of about $45 \pm 10 \mu\text{m}$ can be seen. This is in good agreement with the calculated thickness value of 47.6 μm for a volume fraction of about 5 vol.%, i.e. reduction of a 1 mm thick sheet by 95.23%. Effects from the specific processing conditions appear as strong banding in the case of the massively cold deformed Fe/Fe40Ni material (Fig. 3a, right image) and abnormal grain growth in the outer layers of the Fe2Si/Fe0.2C/Fe2Si bonded material (Fig. 3b, right image). The latter phenomenon is typical for Si-alloyed Fe and exploited, e.g. in electrical steels [42, 43]. Within the limits of the applied characterisation techniques, the interface between both austenitic and martensitic intermediate layers and the surrounding ferrite layers is free from mesoscopic defects such as cracks, pores or oxides.

Results from microstructural characterisation of the Fe/Fe40Ni/Fe hybrid sheet after the final heat treatment are summarised in Fig. 4. The SEM image (Fig. 4a) reveals that the annealing led to recrystallisation of both strongly pre-deformed materials, eliminating the pronounced banding resulting from cold-rolling (Fig. 3a). The sharp chemical gradients of the EDX linescan profile shown in Fig. 4b (measured along the white arrow in Fig. 4a) give no indication of significant Ni interdiffusion across the interface. This retention of the chosen chemical concentrations throughout the bonding and processing procedure leads to the desired multiphase microstructure visualised in the colour coded EBSD maps in Fig. 4c: The phase map (left image; ferrite = red, austenite = green) and inverse pole figure map (right image; for the orientation triangle see Fig. 6b) show a fully austenitic Fe40Ni layer with a sharp interface towards the surrounding ferritic Fe matrix, with random oriented grains for both materials. The extent of recrystallisation appears to be different for both materials: the Fe40Ni layers exhibit a less homogeneous grain size distribution as well as less equiaxed grains compared to the Fe layers, indicating that recrystallisation of Fe40Ni layers is not complete after the annealing treatment.

The production of several layers with different thickness in one bulk sample is demonstrated in Fig. 5. The SEM mi-

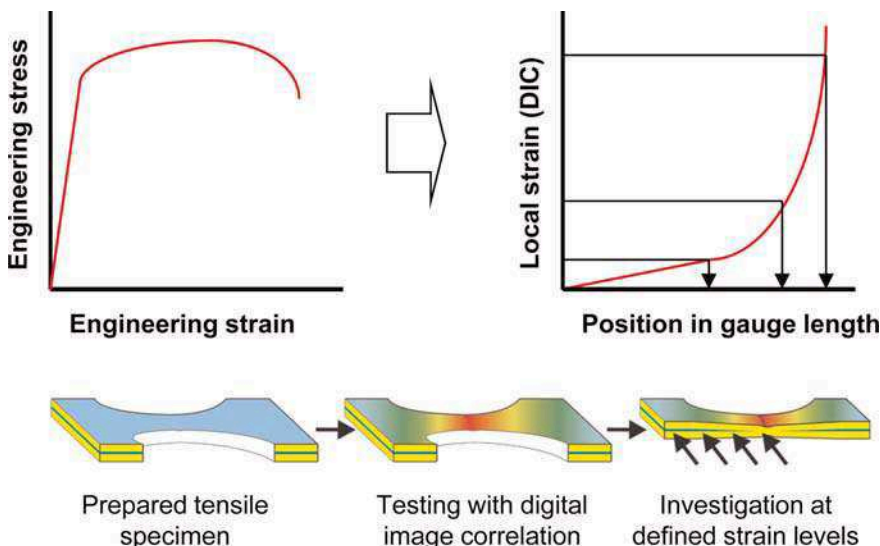


Fig. 2. Sketch of the tensile testing setup for microstructure investigations at regions of different local strains.

crograph (Fig. 5a) and the colour coded EBSD phase map (Fig. 5b) show a ferritic matrix containing four austenitic layers with approximate thickness values of 0.5, 3, 8 and 160 μm (top to bottom), respectively. While the three thicker layers at the bottom are comparable to the single layers shown in Fig. 4, the thinnest layer at the top is barely visible (white arrows in Fig. 5a and b), and higher magnification imaging (Fig. 5c) reveals discontinuities and larger variations in thickness for the thinnest layer.

Respective characterisation results for an Fe₂Si/Fe_{0.2}C/Fe₂Si material compound (with 5 vol.% martensite) after its final heat treatment (annealing and water quenching) are compiled in Fig. 6. In the SEM images (Fig. 6a) and EBSD inverse pole figure maps (Fig. 6b) of different magnifications it can be seen that the intermediate Fe_{0.2}C layer was entirely transformed to martensite (former austenite grain size about 20 μm) while the surrounding Fe₂Si remained ferritic. Despite the comparatively high activity and fast interdiffusion of the interstitial C, sharp chemical gradients remain clearly visible (EPMA linescan profile in Fig. 6c, obtained along the red arrow in Fig. 6a). In conclusion we achieved smooth, straight, and well defined ferrite/

martensite interfaces within the bulk steel sheets, with no mesoscopic defects or shape irregularities observable by SEM analysis (Fig. 6a, right image).

3.2. Mechanical testing of the ferrite–martensite–ferrite compound materials

Micro-hardness measurements showed 217 ± 15 HV_{0.1} for the undeformed ferritic Fe₂Si layers and 560 ± 51 HV_{0.1} for the martensitic Fe_{0.2}C layers. Typical engineering stress–strain curves from tensile testing of the compound materials with different volume fractions of martensite are shown in Fig. 7a together with the respective data for monolithic materials after identical processing. As expected from the hardness values, the compounds' strength increases with martensite fraction while the ductility decreases. The uniform elongation (*UE*) and ultimate tensile strength (*UTS*) follow a hyperbolic relationship with changing martensite thickness, which hints at earlier damage nucleation in thicker martensite layers (Fig. 7b). Yield stress and *UTS* of the different compound materials are in reasonable agreement (about 15%) with values calculated from a

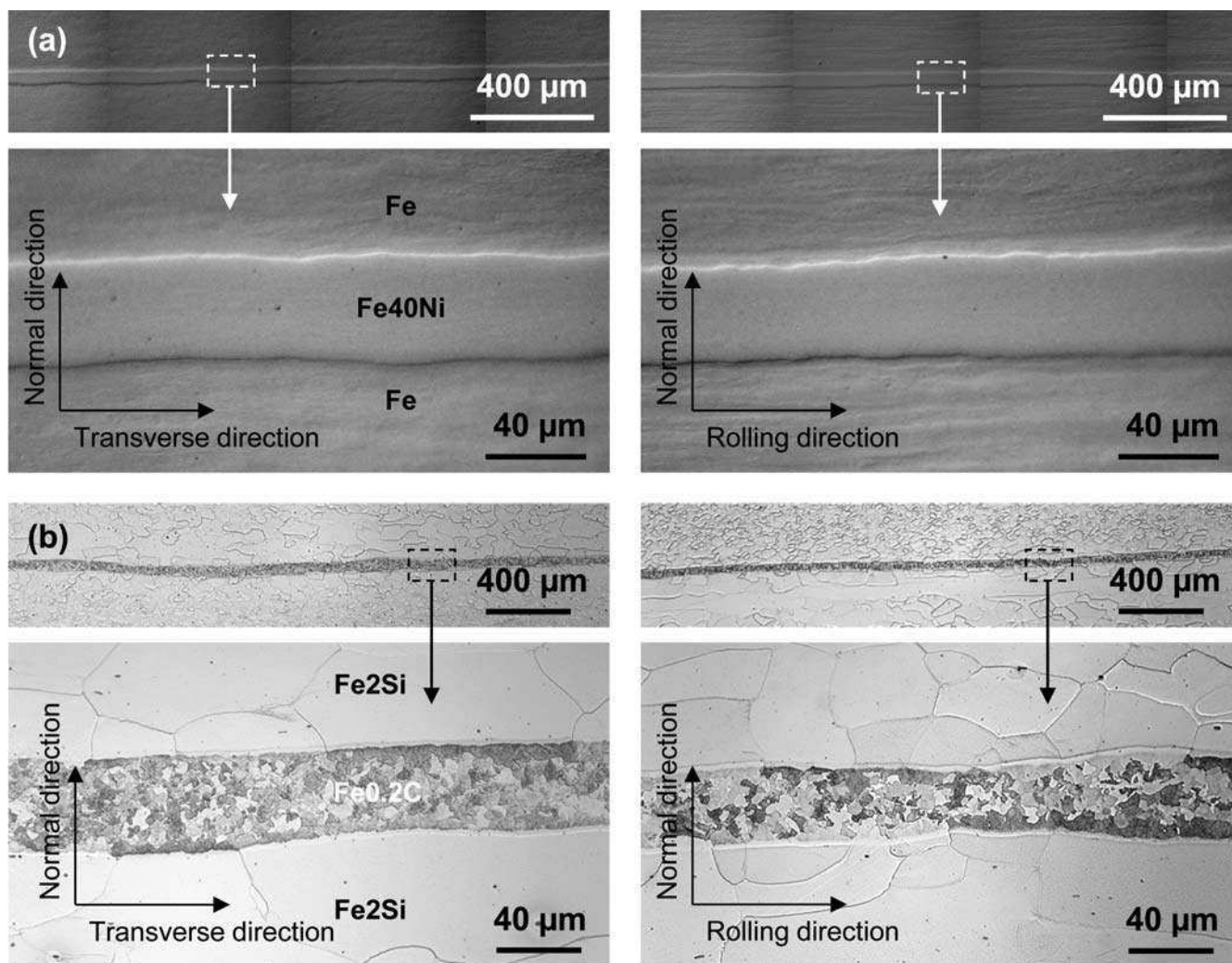


Fig. 3. Optical microscopy investigation on cross-sections (left) and longitudinal sections (right) of the as-processed microstructures before the respective final heat treatments: (a) Fe/Fe₄₀Ni/Fe, (b) Fe₂Si/Fe_{0.2}C/Fe₂Si.

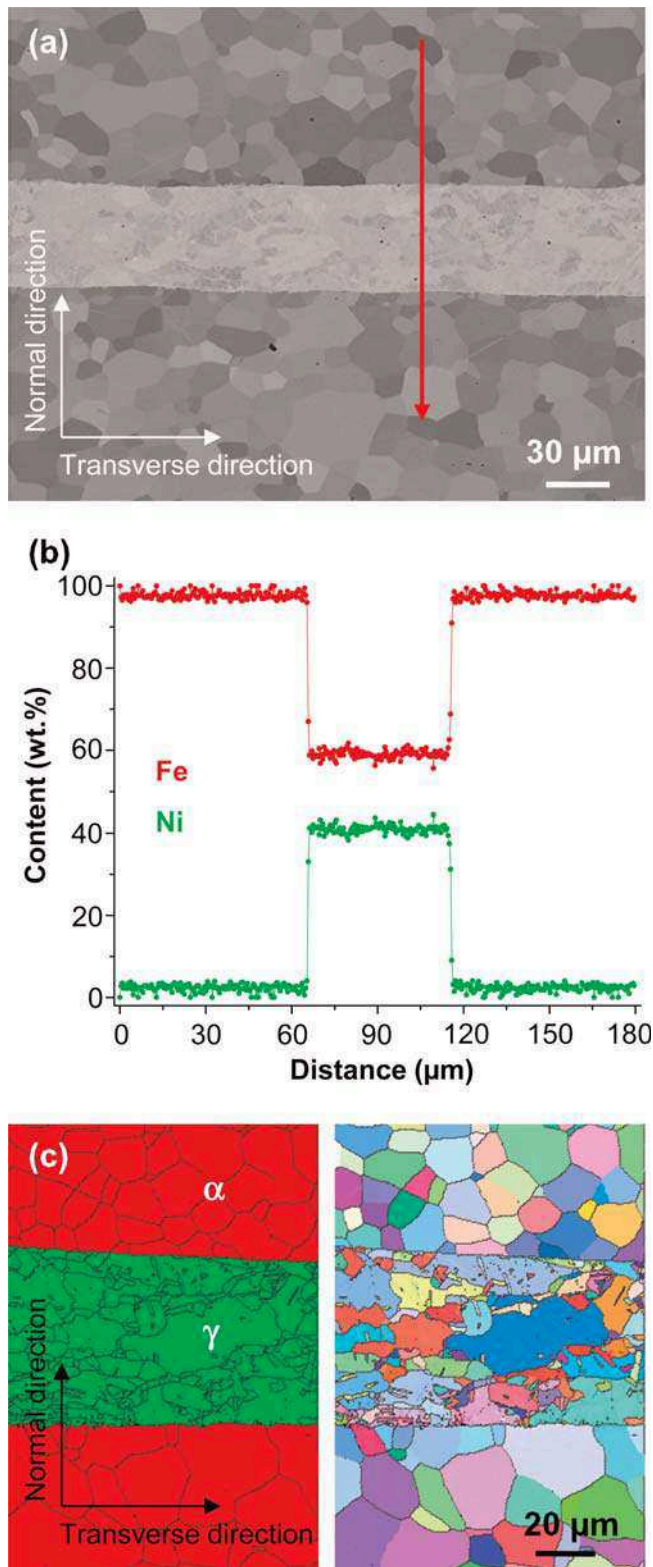


Fig. 4. Scanning electron microscopy investigation of the Fe/Fe40Ni/Fe compound material after the final recrystallisation treatment at 700 °C for 10 min: (a) Backscattered electron contrast image, (b) chemical concentration profiles obtained by EDX measurements along the red arrow in (a), (c) colour coded EBSD phase map showing austenite in green and ferrite in red (left) and inverse pole figure map (right, the corresponding orientation triangle is shown in Fig. 6b).

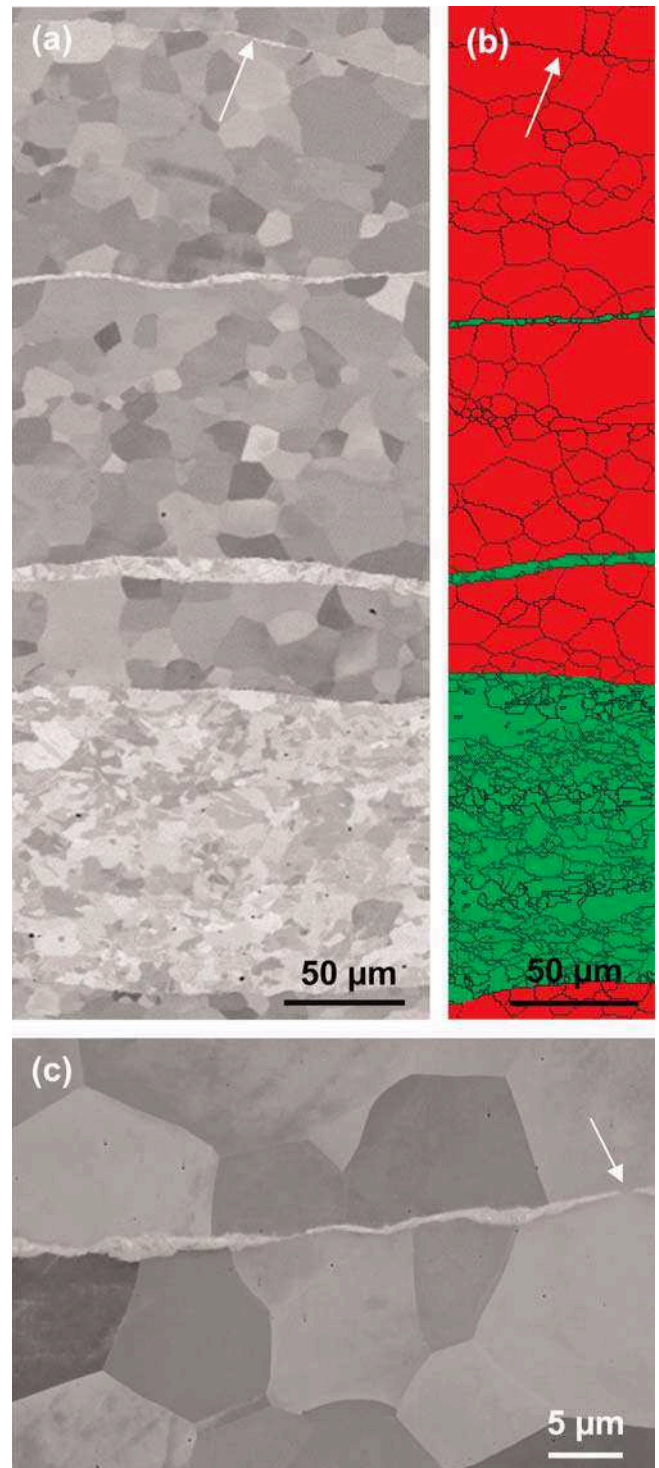


Fig. 5. Scanning electron microscopy investigation of an Fe/Fe40Ni/Fe compound material containing four austenitic layers in a ferritic matrix: (a) Backscattered electron contrast image, (b) colour coded EBSD phase map showing austenite in green and ferrite in red, (c) higher magnification view of (a) showing the thinnest austenitic layer. The white arrows indicate the position of the thinnest austenitic layer in the bulk specimen and onset of its discontinuity, respectively.

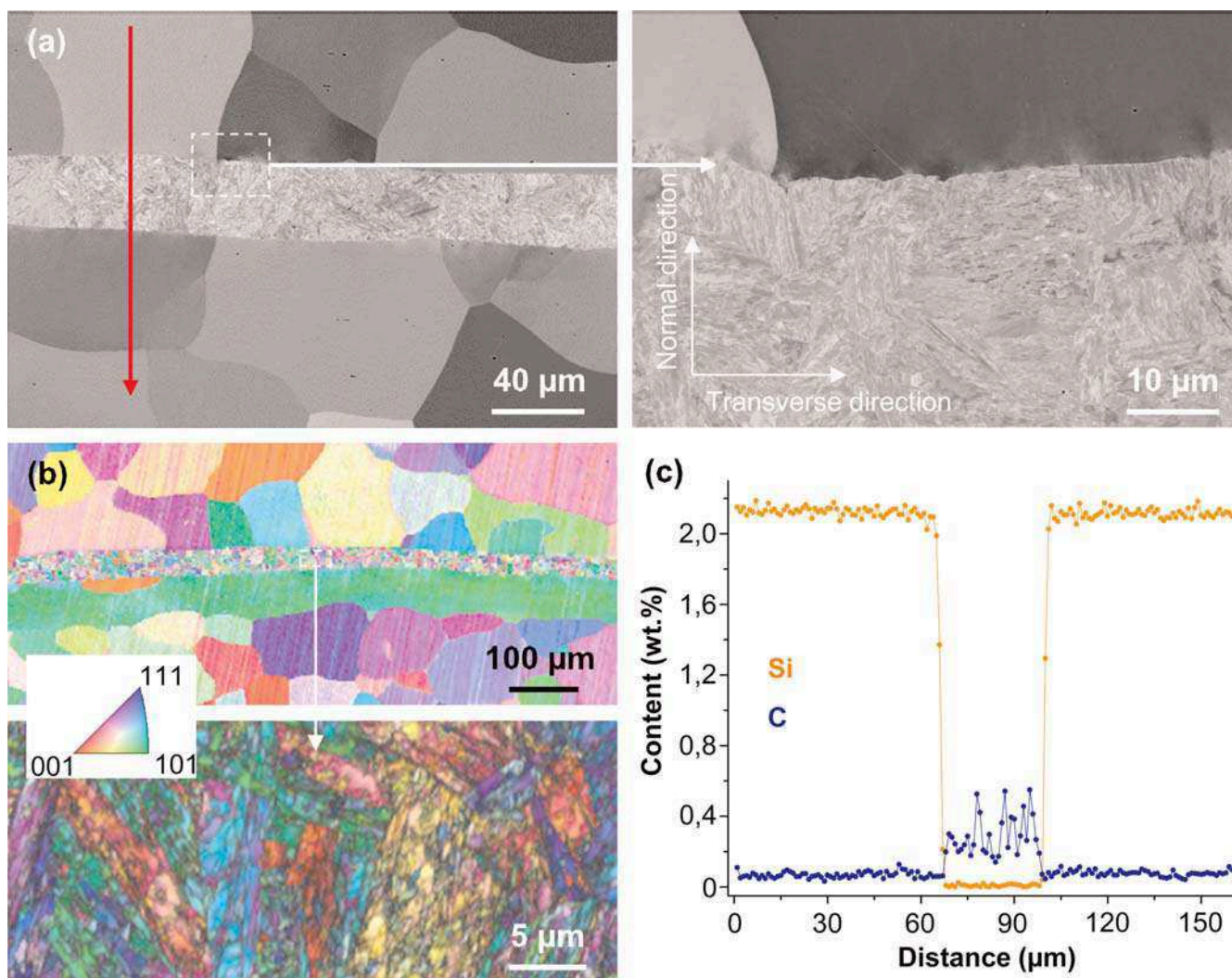


Fig. 6. Scanning electron microscopy investigation of the Fe₂Si/Fe_{0.2}C/Fe₂Si compound material after the final water quenching from 900 °C: (a) Backscattered electron contrast images of different magnification, (b) colour coded EBSD inverse pole figure maps of different magnification, (c) chemical concentration profiles obtained by EPMA measurements along the red arrow in (a).

linear rule of mixtures, while the elongation (total and uniform) is up to 50% less than expected. OM investigations on longitudinal sections (compiled in Fig. 7c) give hints that the compound materials with larger martensite fractions appear to have failed by brittle cleavage of the martensitic layer followed by ductile shearing of the soft surrounding ferrite (about 45° angle towards the tensile axis), similar to what was observed by Inoue et al. [36].

Investigations of the microstructural response and interaction of the two intimately bonded materials of widely differing properties requires, especially for thinner martensitic layers, more detailed investigations. Typical results for a Fe₂Si/Fe_{0.2}C/Fe₂Si tensile specimen with only 5 vol.% martensite are compiled in Fig. 8. Data from local strain measurements on the outer surface obtained by digital image correlation indicate a uniform strain of about 10% just before rupture of the sample, while up to 110% elongation and more were reached in the neck (Fig. 8a). SEM pictures (backscattered electron contrast, Fig. 8b) taken along the corresponding longitudinal section at regions of different local strain reveal the absence of cracks penetrating the

martensite layer (tunnel cracks) and strong formation – increasing with strain – of voids (white arrow pointing down) and shear bands within the ferrite, indicating very high damage tolerance and ductility. Delaminations at the interface between Fe₂Si and Fe_{0.2}C occurred only at the very edge connected to the fractured surface (white arrow pointing up). With increasing strain the thickness of the martensite layer decreases by more than 50%; from about 50 µm to less than 20 µm at the neck, maintaining the thickness ratio to the surrounding ferrite. Parallel with the thinning of the layer, progressively at local strains of 80% and more, the martensite laths seem to align along the tensile axis.

4. Discussion

Bulk multiphase materials of highly controlled geometrical and microstructural morphologies were successfully produced using a thermo-mechanically controlled roll-bonding approach (Figs. 1 and 3). By choosing appropriate bonding and processing parameters for the desired final microstructures, well defined micro-layers ranging from several hun-

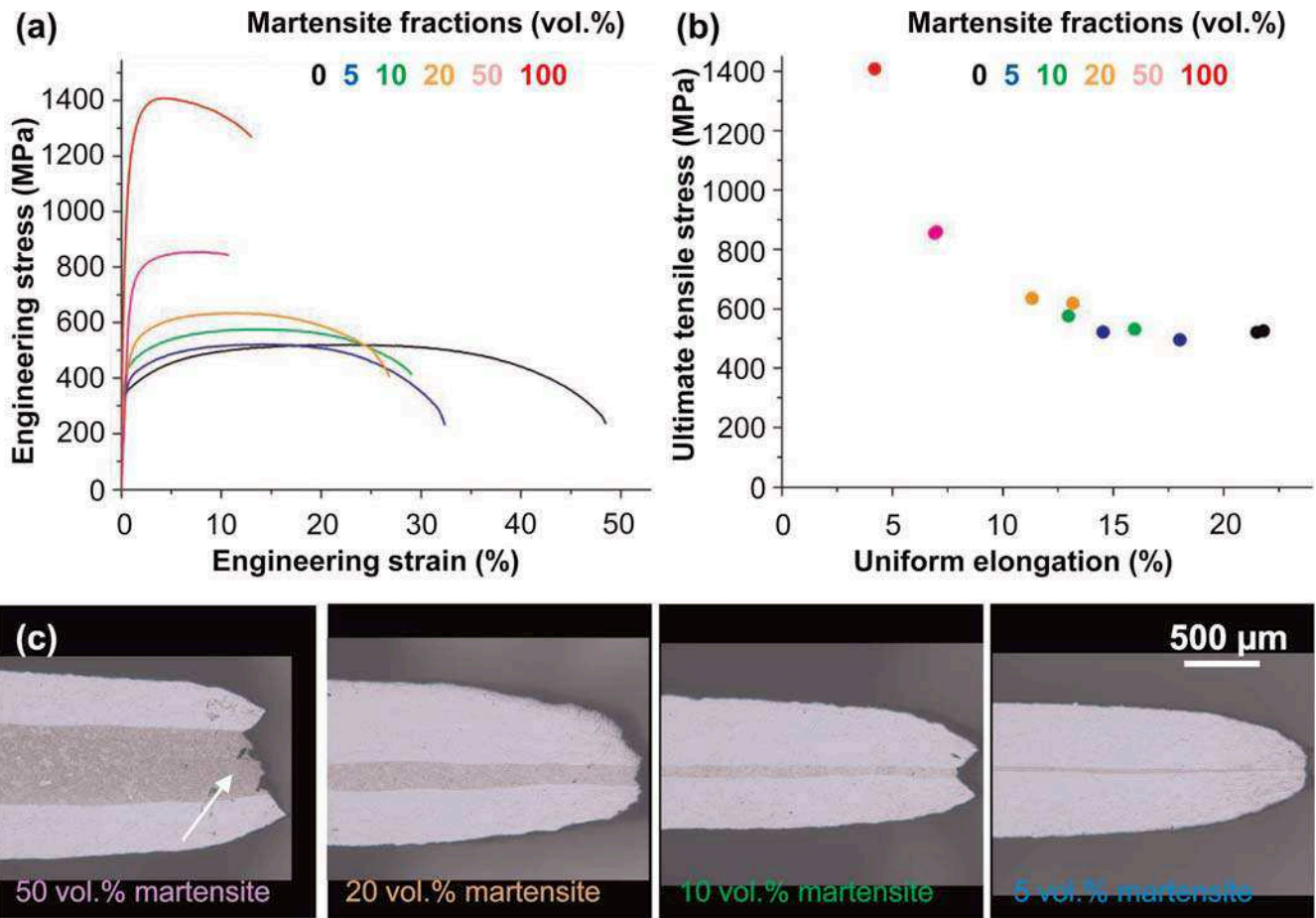


Fig. 7. Mechanical testing of the Fe₂Si/Fe_{0.2}C/Fe₂Si compound materials: (a) Engineering stress–strain curves together with results for the monolithic materials, (b) ultimate tensile strength plotted as a function of the respective uniform elongation reached in tensile testing of compounds with different martensite fractions, (c) optical micrographs of longitudinal sections after tensile testing; the white arrow indicates subcracks in the martensitic layer of 50% volume fraction.

dred μm down to less than 1 μm of austenite and martensite, respectively, were produced in bulk ferrite matrices. Ferrite, austenite and martensite represent the most frequently employed secondary constituents in high strength steels [1–3]. Of special importance for producing layer interfaces of high geometrical precision appears to be the selection of the respective optimum temperatures, in order to minimise the thermodynamic driving forces for interdiffusion, thus suppressing the undesired formation of additional phases and or a blurred interface (Figs. 4 and 6).

While layers of 20 μm thickness and above could be readily synthesised and tested, the design of even thinner layers is not only of great interest related to changes in the mechanical properties, but also to allow controlled studies of the nano-scaled components present in advanced structural materials [14–16, 44]. The lowest bound in layer thickness (austenite or martensite, respectively) we reached is about 1 μm. Around and below this value the geometrical precision as well as the interface quality start to degrade and the layers begin to break up (Fig. 5). This mainly results from the then necessary multiple (or accumulative) bonding passes, where the already closely joined sheets are reheated to the bonding temperature of 1 100 °C, which renders the material briefly above the optimum temperature for limited interdiffusion (Fig. 1). This may be overcome by

using lower bonding temperatures, compensated by the adaptation of other parameters for each specific material combination (i. e. increased rolling reduction) to ensure sufficient bonding strength and interface quality. Alternatively, materials with an even more pronounced initial thickness ratio may be deployed, thus eliminating the need for multiple bonding. This may be done by using, e. g. melt-spun ribbons or even coatings for the layers instead of sheet metal [45], and/or much thicker blocks as outer “matrix” materials. Rolling further to sheet dimensions below about 1 mm thickness is not favourable in view of sample handling, heat treating and testing robustness. The geometrical precision of the layered structure may be further improved by the respective sample preparation; i. e. polished bonding surfaces instead of ground ones, as well as extra smooth rolls. Nevertheless, even with the current setup, nano-sized layers can be produced and investigated, as it is readily possible to select suitable areas of interest along the large sample. The current value of centre-layers with more homogeneous properties and topology having thicknesses down to about 1 μm is an excellent example though for studying the micromechanics of ultrafine grained multiphase steels [4, 14].

Most studies concerned with multilayered materials aim at improving the overall mechanical and/or physical prop-

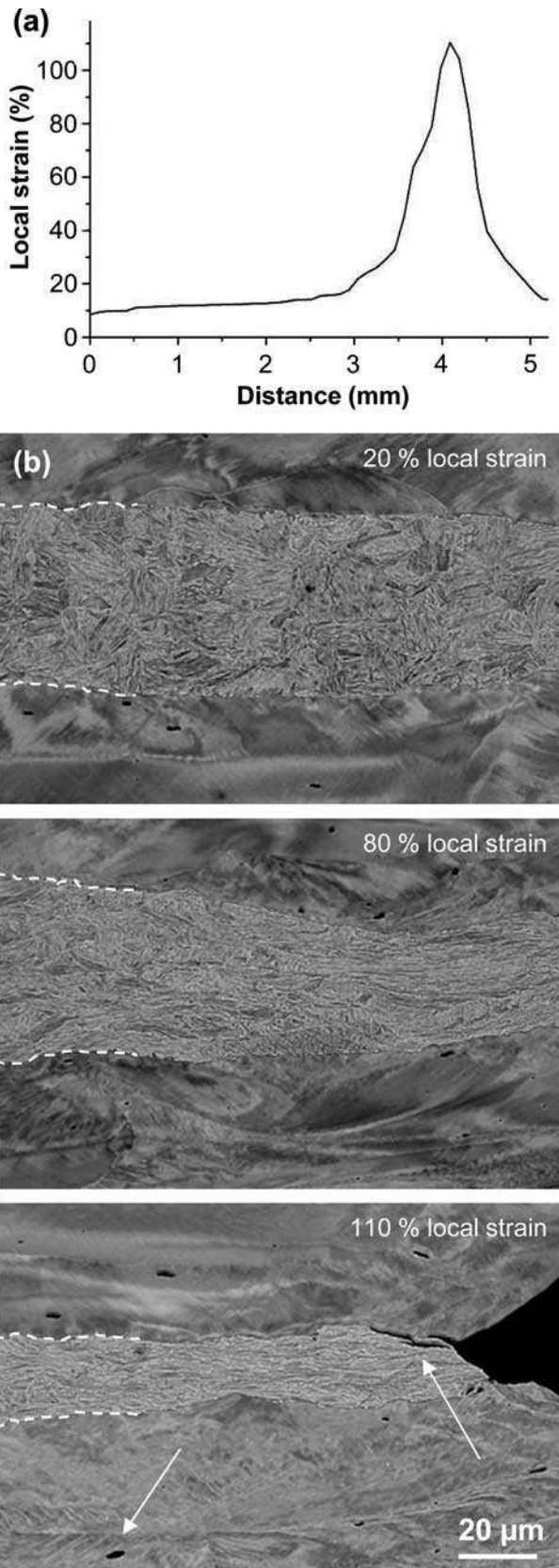


Fig. 8. More detailed analysis of the co-deformation processes of a Fe₂Si/Fe_{0.2}C/Fe₂Si compound with 5 vol.% martensite fraction: (a) Local strain on the rolling plain of the Fe₂Si/Fe_{0.2}C/Fe₂Si specimen obtained by digital image correlation just before rupture in the tensile test, (b) backscattered electron contrast images taken at different local strain regions; the white arrows indicate beginning delamination (arrow pointing up) and void formation in ferrite (arrow pointing down), respectively.

erties, and the to-be-combined materials are chosen accordingly [33, 37, 46–49]. The goal is – irrespective of the chosen synthesis technique – to overcome typical inverse relationships observed for monolithic structural materials, such as between strength and ductility [20, 48], or eliminate specific weaknesses, such as low corrosion [50] or wear resistance [49]. In most cases, applicability of a linear rule of mixtures is reported for the mechanical properties of hybrid materials; meaning that, e.g. the strength of the bonded sheet lies between the values of the components in linear relation to their respective (volume) fractions [20, 21]. With decreasing layer thickness, though, unique properties and combinations thereof have been observed not only for bulk multi-material sheets [38, 51, 52], but also for the constituting layers itself [33, 37, 48]. Such effects can also be observed in “natural” hybrid material such as pearlite, which may be regarded as an in-situ synthesised nano-structured metal-matrix-composite consisting of hard cementite lamellas co-deforming with a soft ferritic matrix e.g. during wire drawing [53–55].

In the present study, we find similar behaviour for the martensite/ferrite compound material, namely that the strong but comparatively brittle martensite can surprisingly be strained to a regime far above the ductility limit of the monolithic Fe_{0.2}C material, when it is embedded in the more ductile ferritic matrix (Figs. 7 and 8), especially for layers thinner than about 100 μm. Inoue et al. [36] observed a similarly increased ductility phenomenon which they explained with an increased uniform elongation of the martensitic layer, made possible by prevented tunnel cracking and hence delayed instability with decreasing layer thickness, which changed the fracture behaviour from brittle cleavage to ductile shearing. The underlying microstructural phenomena were investigated by Nambu et al. [37], who observed a change in the deformation mode of the martensitic layer, i.e. the activation of slip systems outside of the martensite laths and the appearance of transgranular slip bands above a true strain of about 20%. Jeong et al. [56] on the other hand related such an increase in ductility to a change in the stress state of the layers and the gradient between them, caused by constrained necking of martensite through the surrounding austenite. Both explanations are based on data obtained from multilayered sheets made with low C martensitic steel clad with austenitic stainless steel. The respective phenomena within the Fe₂Si/Fe_{0.2}C/Fe₂Si compound materials are the subject of future investigations, aimed at optimising DP steels using this simplified model microstructure. It is therefore a good example of how the combined synthesis and testing approach shown in this study – most ideally also supplemented by modelling – allows for efficient development of novel structural materials. Examples of possible experimental set-ups for the systematic and independent variation and investigation of factors influencing martensite plasticity within ferrite are sketched in Fig. 9.

The basic synthesis and testing setup presented here may be expanded, e.g. to fracture toughness experiments using compact tension specimens or to fatigue studies, most effectively deployed on samples containing different layer thicknesses (Fig. 5). The bonded interface appears to be sufficiently strong to allow for such crack propagation experiments, as no peeling could be observed (Fig. 8b). More than two microstructure components could be investigated

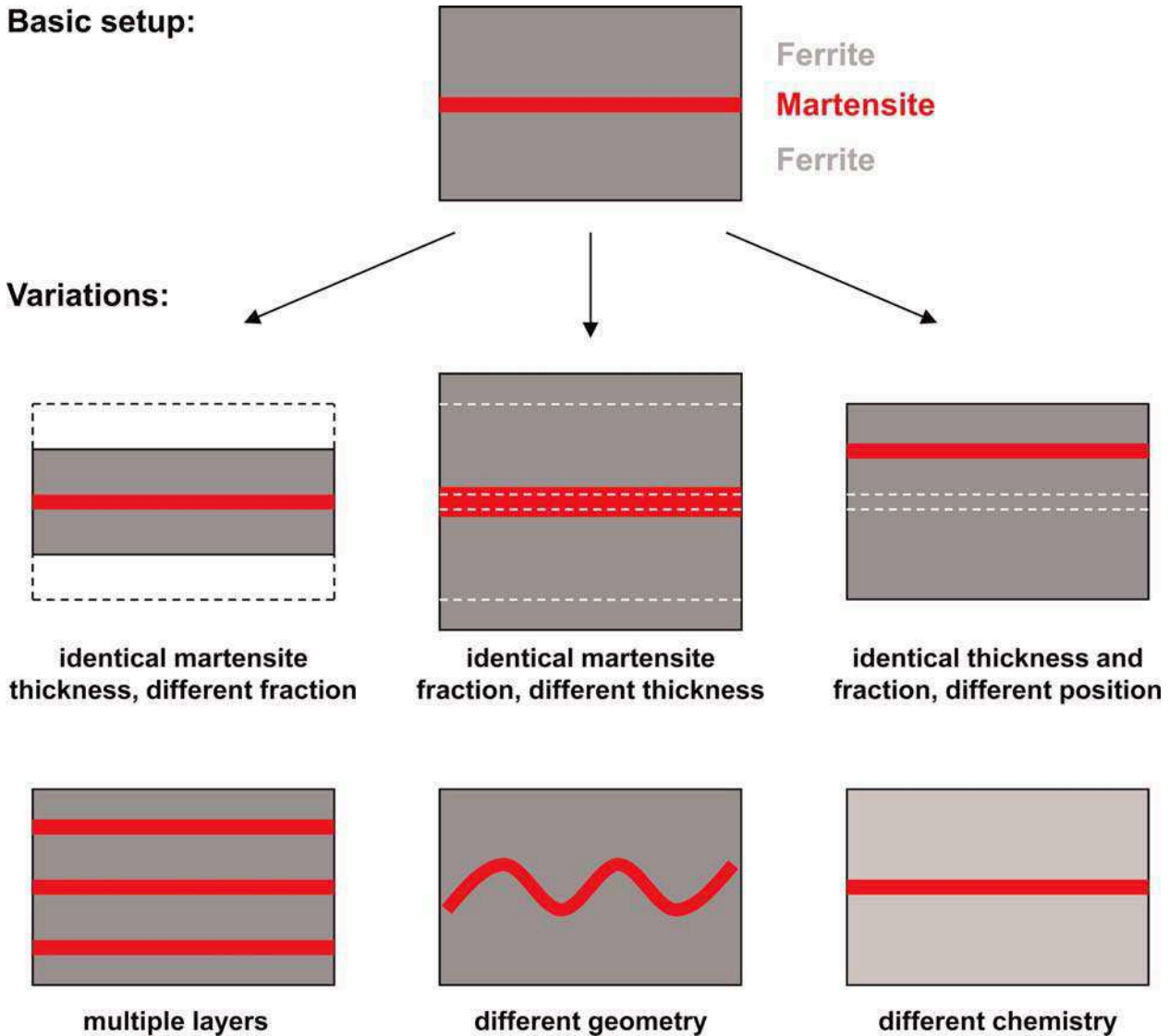


Fig. 9. Possible future investigations to optimise dual-phase steel microstructures using the presented methodology: sketches of experimental setups for the systematic and independent variation of factors influencing martensite plasticity within ferrite.

not only by combining materials of respective chemical compositions, but also by the utilisation of diffusion (“up-hill” or “down-hill”) across the interface as an additional parameter for the thermo-mechanically controlled synthesis. Apart from the targeted investigation of microstructural constituents and their mutual interaction, the presented approach may also be used for the top-down design of novel hybrid materials, which otherwise would need extremely difficult annealing or solidification routes [20, 21]. Material systems other than Fe-base, such as titanium or aluminium alloys, may require adapted bonding preparations and parameters.

5. Summary and conclusions

We present a new approach for the targeted design and analysis of second phase microstructural components present in structural materials. The method allows for investigating individual phase behaviour and interaction during deforma-

tion. The approach consists of a thermo-mechanically controlled roll-bonding procedure for creating bulk multi-layered sheets, coupled with a characterisation routine for tracking the local deformation during mechanical testing. Two examples for such geometrically simplified model microstructures, resembling strongly partitioned dual and duplex phase steels, were chosen to demonstrate the effectiveness of the method: Ferrite/austenite/ferrite compounds were created by bonding Fe-40 wt.% Ni between blocks of Fe, martensitic layers within a ferritic matrix were obtained by joining Fe-0.2 wt.% C with Fe-2 wt.% Si. The main conclusions are:

1. By controlling the thermo-mechanical parameters during bonding and processing, especially temperatures, interdiffusion across the joint interfaces could be minimised, which results in sharp chemical gradients as well as micro-scaled layers of even thickness and with no apparent interfacial defects.
2. Using the current bonding procedure, the lower limit was found at about 1 μm layer thickness within a 1 mm

- thick bulk steel sheet. Nano-sized layers could be produced but of reduced quality. Creating sub-micron layers without sacrificing geometrical and interfacial quality may be achieved by larger initial thickness ratios between the chosen materials and/or adapted bonding parameters.
3. Non-tempered 0.2 wt.% C martensite with a microhardness of about 560 HV0.1 and about 15 % tensile elongation at fracture as a monolithic material could be deformed to more than 110% local elongation when encased as a 50 µm thick layer in a 1 mm thick ferritic sheet. Ongoing investigations aim at a systematic variation of martensite thickness and corresponding high resolution analysis of the deformation behaviour and interfacial phenomena, to elucidate the mechanisms promoting martensite plasticity.
 4. Our approach enables producing model microstructures of reduced complexity for the targeted analysis of multi-phase deformation phenomena, e.g. strain partitioning and localisation, crack arresting or slip-transitions. It represents a link between complex bulk microstructure investigations and highly precise micro-mechanical testing methods, and thus contributes to more efficient and knowledge-based alloy design of structural materials.
 5. Future developments are concerned with broadening the scope of the procedure, namely
 - optimising thermo-mechanical parameters for thinner layers or with different geometries such as waves,
 - implementing metalloid phases such as carbides,
 - developing other testing setups like micro-crack-propagation experiments, and, most importantly,
 - combining it with corresponding microstructure modelling tools.

M. Wang, D. Yan and M. Adamek are acknowledged for assisting in microstructure characterisation and mechanical testing.

References

- [1] H.K.D.H. Bhadeshia, R. Honeycombe: *Steels, Microstructure and Properties*, 3rd Ed. Elsevier, Oxford, UK (2006).
- [2] H. Berns, W. Theisen: *Eisenwerkstoffe Stahl und Gusseisen*, Springer Verlag Berlin, Heidelberg (2006).
- [3] M.F. Ashby: *Materials Selection in Mechanical Design*, Butterworth-Heinemann, Burlington, MA, USA (2005).
- [4] M. Calcagnotto, D. Ponge, D. Raabe: *Mater. Sci. Eng. A* 527 (2010) 7832–7840. DOI:10.1016/j.msea.2010.01.004
- [5] D. Raabe, D. Ponge, O. Dmitrieva, B. Sander: *Scr. Mater.* 60 (2009) 1141–1144. DOI:10.1016/j.scriptamat.2009.02.062
- [6] C. Herrera, D. Ponge, D. Raabe: *Acta Mater.* 59 (2011) 4653–4664. DOI:10.1016/j.actamat.2011.04.011
- [7] O. Bouaziza, S. Allaina, C.P. Scotta, P. Cugya, D. Barbier: *Curr. Opin. Solid State Mater. Sci.* 15 (2011) 141–168. DOI:10.1016/j.cossms.2011.04.002
- [8] G. Frommeyer, U. Brüx: *Steel Res. Int.* 77 (2006) 627–633.
- [9] U. Dilthey, L. Stein: *Sci. Technol. Weld. Joining* 11 (2006) 135. DOI:10.1179/174329306X85967
- [10] J. Speer, D.K. Matlock, B.C. De Cooman, J.G. Schroth: *Acta Mater.* 51 (2003) 2611–2622. DOI:10.1016/S1359-6454(03)00059-4
- [11] J.G. Speer, D.V. Edmonds, F.C. Rizzo, D.K. Matlock: *Curr. Opin. Solid State Mater. Sci.* 8 (2004) 219–237. DOI:10.1016/j.cossms.2004.09.003
- [12] G. Gottstein: *Physical Foundations of Materials Science*. Springer Verlag Berlin (2004). DOI:10.1007/978-3-662-09291-0
- [13] N.J. Kim, G. Thomas: *Met. Trans. A* 12 (1981) 483. DOI:10.1007/BF02643691
- [14] M. Calcagnotto, D. Ponge, E. Demir, D. Raabe: *Mater. Sci. Eng. A* 527 (2010) 2738–2746. DOI:10.1016/j.msea.2010.01.004
- [15] H. Springer, M. Belde, D. Raabe: *Mater. Sci. Eng. A* 582 (2013) 235–244. DOI:10.1016/j.msea.2013.06.036
- [16] L. Yuan, D. Ponge, J. Wittig, P. Choi, J.A. Jiménez, D. Raabe: *Acta Mater.* 60 (2012) 2790–2804. DOI:10.1016/j.actamat.2011.11.042
- [17] J.R. Greer, J.Y. Kim, M.J. Burke: *JOM* 61 12 (2009) 19–25. DOI:10.1007/s11837-009-0174-8
- [18] O. Kraft, C.A. Volkert: *Adv. Eng. Mater.* 3 (2001) 99–110. DOI:10.1002/1527-2648(200103)3:3<99::AID-ADEM99>3.0.CO;2-2
- [19] C.C. Tasan, J.P.M. Hoefnagels, M.G.D. Geers: *Scr. Mater.* 63 (2010) 835–838. DOI:10.1016/j.scriptamat.2010.02.014
- [20] D.R. Lesuer, C.K. Syn, O.D. Sherby, J. Wadsworth, J.J. Lewandowski, W.H. Hunt Jr.: *Int. Mater. Rev.* 41 (1996) 5, 169. DOI:10.1179/imr.1996.41.5.169
- [21] D. Embury, O. Bouaziz: *Annu. Rev. Mater. Res.* 40 (2010) 213. DOI:10.1146/annurev-matsci-070909-104438
- [22] N.A. Mara, D. Bhattacharyya, P. Dickerson, R.G. Hoagland, A. Misra: *Appl. Phys. Lett.* 92 (2008) 231901. DOI:10.1063/1.2938921
- [23] J. Emmerlich, D. Music, M. Braun, P. Fayek, F. Munnik, J.M. Schneider: *J. Phys. D: Appl. Phys.* 42 (2009) 6. DOI:10.1088/0022-3727/42/18/185406
- [24] S. Chatterjee, T.K. Pal: *Wear* 255 (2003) 417–425. DOI:10.1016/S0043-1648(03)00101-7
- [25] M.F. Buchely, J.C. Gutierrez, L.M. León, A. Toro: *Wear* 259 (2005) 52. DOI:10.1016/j.wear.2005.03.002
- [26] D.S. Gnanamuthu: *Opt. Eng.* 19 (1980) 783. DOI:10.1117/12.7972604
- [27] X. Zhang, N. Hansen, Y. Gao, X. Huang: *Acta Mater.* 60 (2012) 5933–5943. DOI:10.1016/j.actamat.2011.09.008
- [28] I.J. Beyerlein, N.A. Mara, J. Wang, J.S. Carpenter, S.J. Zheng, W.Z. Han, R.F. Zhang, K. Kang, T. Nizolek, T.M. Pollock: *JOM* 64 (2012) 10. DOI:10.1007/s11837-012-0431-0
- [29] S. Zheng, I. Beyerlein, J.S. Carpenter, K. Kang, J. Wang, W. Han, N.A. Mara: *Nature Com.* 4 (2013) 1969.
- [30] S. Roy, B.R. Nataraj, S. Suwas, S. Kumar, K. Chattopadhyay: *Mater. Des.* 36 (2012) 529. DOI:10.1016/j.matdes.2011.11.015
- [31] N. Tsuji, Y. Saito, Y. Minamino: *Scr. Mater.* 47 (2002) 893. DOI:10.1016/S1359-6462(02)00088-X
- [32] L. Li, K. Nagai, F. Yin: *Sci. Technol. Adv. Mater.* 9 (2008) 11. DOI:10.1088/1468-6996/9/2/023001
- [33] S. Nambu, M. Michiuchi, J. Inoue, T. Koseki: *Comp. Sci. Technol.* 69 (2009) 1936. DOI:10.1016/j.compscitech.2009.04.013
- [34] M.J. Rathod, M. Kutsuna: *Weld. Res.* 16 (2004) 26.
- [35] F.H. Milanez, M.B.H. Mantelli: *Int. J. Heat Mass Transfer* 46 (2003) 4573. DOI:10.1016/S0017-9310(03)00294-1
- [36] J. Inoue, S. Nambu, Y. Ishimoto, T. Koseki: *Scr. Mater.* 59 (2008) 1055. DOI:10.1016/j.scriptamat.2008.07.020
- [37] S. Nambu, M. Michiuchi, Y. Ishimoto, K. Asakura, J. Inoue, T. Koseki: *Scr. Mater.* 60 (2009) 221. DOI:10.1016/j.scriptamat.2008.10.007
- [38] T.A. Wynna, D. Bhattacharyya, N.A. Mara: *Mater. Sci. Eng. A* 564 (2013) 213. DOI:10.1016/j.msea.2012.11.114
- [39] M. Eizadjou, H. Danesh Manesh, K. Janghorban: *Mater. Des.* 29 (2008) 909. DOI:10.1016/j.matdes.2007.03.020
- [40] L.S. Darken: *Trans. AIME, TP2443, Metals Technology* (1948) 430.
- [41] R. Bernst, G. Inden, A. Schneider: *Calphad.* 32 (2008) 207. DOI:10.1016/j.calphad.2008.02.002
- [42] Y. Hayakawa, J.A. Szpunars: *Acta Mater.* 45 (1997) 11, 4713. DOI:10.1016/S1359-6454(96)00251-0
- [43] Z. Xia, Y. Kang, Q. Wang: *J. Magn. Mater.* 320 (2008) 3229. DOI:10.1016/j.jmmm.2007.06.010
- [44] H. Springer, D. Raabe: *Acta Mater.* 60 (2012) 4950. DOI:10.1016/j.actamat.2012.05.017
- [45] R. Jamaati, M.R. Toroghinejad: *Mater. Des.* 31 (2010) 4816. DOI:10.1016/j.matdes.2010.04.022
- [46] O.M. Abdelhadi, L. Ladani, J. Razmi: *Mech. Mater.* 43 (2011) 885. DOI:10.1016/j.mechmat.2011.09.006
- [47] A. Tasdemirci, I.W. Hall: *Mater. Des.* 30 (2009) 1533. DOI:10.1016/j.matdes.2008.07.054
- [48] J. Yanagimoto, T. Oya, S. Kawanishi, N. Tiesler, T. Koseki: *CIRP Annals – Manufact. Technol.* 59 (2010) 287. DOI:10.1016/j.cirp.2010.03.109

- [49] C.W. Lee, J.H. Han, J. Yoon, M.C. Shin, S.I. Kwun: Surf. Coat. Technol. 204 (2010) 2223–2229.
DOI:10.1016/j.surfcoat.2009.12.014
- [50] M. Göken, H.W. Höppel: Adv. Mater. 23 (2011) 2663.
DOI:10.1002/adma.201100407
- [51] Y. Liu, D. Bufford, H. Wang, C. Sun, X. Zhang: Acta Mater. 59 (2011) 1924. DOI:10.1016/j.actamat.2010.10.052
- [52] B. Ham, X. Zhang: Mater. Sci. Eng. A 528 (2011) 2028.
DOI:10.1016/j.msea.2010.10.101
- [53] J.D. Embury, R.M. Fisher: Acta Metall. 14 (1966) 147.
DOI:10.1016/0001-6160(66)90296-3
- [54] D. Raabe, P.P. Choi, Y.J. Li, A. Kostka, X. Sauvage, F. Lecourturier, K. Hono, R. Kirchheim, R. Pippan, D. Embury: MRS Bull. 35 (2010) 982. DOI:10.1557/mrs2010.703
- [55] Y.J. Li, P.P. Choi, C. Borchers, S. Westerkamp, S. Goto, D. Raabe, R. Kirchheim: Acta Mater. 59 (2011) 3965.
DOI:10.1016/j.actamat.2010.08.015
- [56] C. Jeonga, T. Oyab, J. Yanagimoto: J. Mater. Process. Technol. 213 (2013) 614. DOI:10.1016/j.jmatprotec.2012.10.017

(Received May 12, 2014; accepted August 15, 2014; online since November 24, 2014)

Correspondence address

Dr. Hauke Springer
Max-Planck-Institut für Eisenforschung GmbH
Max-Planck-Straße 1
40237 Düsseldorf
Germany
Tel.: +49 211 6792 796
Fax: +49 211 6792 333
E-mail: h.springer@mpie.de

Bibliography

DOI 10.3139/146.111156
Int. J. Mater. Res. (formerly Z. Metallkd.)
106 (2015) 1; page 3–14
© Carl Hanser Verlag GmbH & Co. KG
ISSN 1862-5282